HIGH RESOLUTION SPECTROSCOPY
OF THE VAN DER WAALS MOLECULES NaAr AND NaKr*

D. Zimmermann

Institute for Radiation and Nuclear Physics
Technical University Berlin
D-1000 Berlin 12, Germany

(Received 21 December 1988)

The rovibrational structure of the transition $A^2\Pi - X^2\Sigma$ of the van der Waals molecules NaAr and NaKr has been investigated by means of high resolution laser spectroscopy applying the techniques of laser-induced fluorescence and of optical–optical double resonance to the molecules in a supersonic beam. Precise values for the parameters of rotation have been obtained for the $X^2\Sigma$ state of NaKr^{84}. By means of an investigation of the spectral distribution of the fluorescence light the repulsive part of the $X\Sigma$-potential of NaKr has been determined. Local perturbations have been detected in the $A^2\Pi$ states of both NaAr and NaKr and a full deperturbation analysis has been performed.

1. Introduction

The interaction potential between an alkali atom and a rare gas atom has been the topic of many investigations, both experimentally and theoretically, for a long time. One of the reasons for this continuous interest is the relative simplicity of the system containing only one electron outside closed shells. Therefore, a useful approach to the theoretical calculation is a treatment as a three-body problem consisting of the valence electron, the core of the alkali ion and the rare gas atom. In this way, pseudo potentials or model potentials have been derived for all combinations of an alkali atom with a rare gas atom. Up to now, experimental information on these systems comes mainly from scattering experiments and from line broadening investigations. However, spectroscopic work on diatomic alkali-rare gas van der Waals molecules is expected to provide more precise information on the interaction potentials.

The present contribution deals with the laserspectroscopic investigation of the molecules NaKr and NaAr. The molecular ground state $X^2\Sigma^+$ is weakly bound with a well-depth of the order of 50 cm^{-1}. The first excited P-state of the sodium atom leads to the two excited molecular states $A^2\Pi_{1/2}$ and $A^2\Pi_{3/2}$ with a well-depth of typically 500 cm^{-1} and to the $B^2\Sigma^+$ state. Up to now, only the transition $A\Pi - X\Sigma$ has been studied in detail. The equilibrium distances in the molecular

ground state and in the $A\Pi$ state are quite different. Therefore, starting from the vibrational ground state $v'' = 0$ one can excite only vibrational levels of the $A\Pi$ state around $v' = 10$ with sufficient intensity due to the Franck–Condon principle.

The intention of the present investigation is to contribute to a precise determination of the $X\Sigma$ and of the $A\Pi$ interaction potential. In addition, the results of our investigations may serve as a sensitive test for the accuracy of model potential calculations. As previous results have been published for NaAr [1] and NaKr [2] I restrict myself to the presentation of some new and unpublished material. This work has been performed in cooperation with my coworkers Dr. E. Zanger, Dipl.-Phys. A. Nunnemann, N. Ahr, I. Kapetanakis and V. Schmatloch.

2. Experimental observation and rotational analysis

The van der Waals molecules were produced by supersonic expansion of a mixture of rare gas and sodium vapour through a nozzle into a vacuum. The molecular beam was crossed by the light beam of a tunable single-mode cw dye laser under right angle. The fluorescence light of the molecules was observed in the direction perpendicular to the laser beam and to the jet. The dye laser was electronically scanned under computer control over a wavenumber range of $1\,\mathrm{cm^{-1}}$. The relative frequency of the laser was determined by a Fabry–Perot interferometer, the absolute wavenumber was obtained by recording the well-known absorption lines of the iodine molecule. The intensity of the ·fluorescence light and the transmitted intensities of the Fabry–Perot interferometer and the iodine cell were read by the computer and stored in proper files on the disk for further analysis.

The largest amount of information comes from an investigation of the rovibrational structure of the absorption spectrum of the molecules due to the transition $A\Pi$–$X\Sigma$ where the total intensity of the laser-induced fluorescence is detected. The molecular ground state $X^2\Sigma^+$ is a Hund's coupling case b whereas the $A\Pi$ state is dominantly case a. The small amount of decoupling in the $A\Pi$ state for higher rotational quantum numbers has been taken into account in our analysis. The spin–rotation splitting in the $X\Sigma$ state seems to be smaller than the resolution of our apparatus and could not be observed. Therefore, the rotational structure of each vibrational transition consists of 4 instead of 6 branches: P_1, Q_1, R_1, P_{12} with relative intensities of approximately 3:3:1:1 for $A\Pi_{1/2}$–$X\Sigma$, and P_2, Q_2, R_2, R_{21} with relative intensities of 1:3:3:1 for $A\Pi_{3/2}$–$X\Sigma$. As the hyperfine structure of the sodium atom in its ground state is transferred to the molecular $X\Sigma$ state without change in our case, each rovibrational molecular line appears as a doublet with intensity ratio 5:3 and a splitting of $0.059\,\mathrm{cm^{-1}}$.

Fig. 1 shows as an example one high-resolution scan of the absorption spectrum of NaKr. Due to the strong overlapping of different vibrational bands and due to the presence of several Kr-isotopes in natural mixture the observed absorption spectrum turned out to be highly congested. An assignment of rotational branches and rotational quantum numbers to the numerous absorption lines seems to be very difficult or even impossible without additional experimental information.
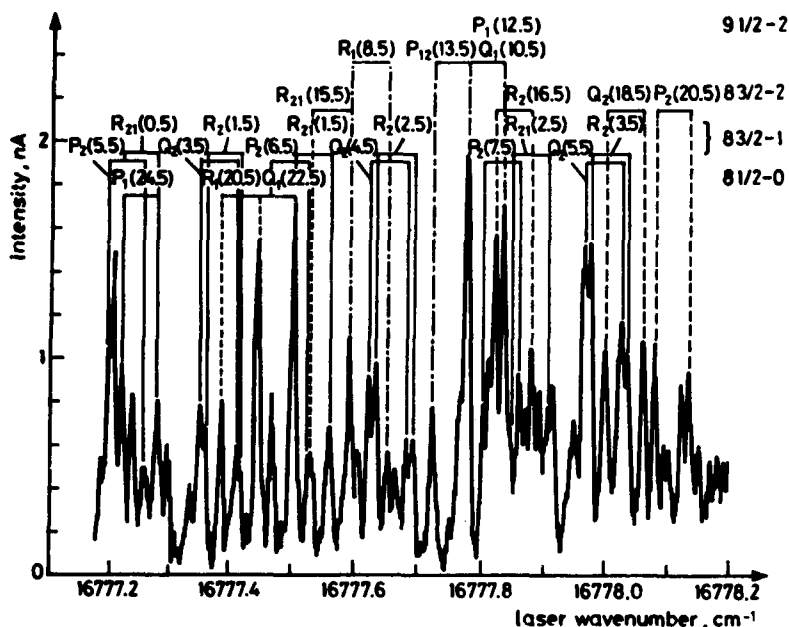
Fig. 1. Part of the high resolution absorption spectrum of NaKr with rotational assignment $P_1(J'')$, $Q_1(J'')$ .... The vibrational assignment in the right upper corner is $v'\Omega - v''$ with $\Omega = 1/2$ and $3/2$ for $A\Pi_{1/2}$ and $A\Pi_{3/2}$ resp.

Therefore, we have applied the method of optical–optical double resonance (OODR) using two tunable single-mode dye lasers of about equal intensity. The frequency of laser B is tuned to a certain rovibronic transition of NaKr while the frequency of laser A is scanned. Both laser beams are chopped with different frequencies f_A and f_B. Our detection scheme for OODR essentially corresponds to an observation of the part of the fluorescence light being modulated with frequency $f_A + f_B$. Under these conditions we can observe OODR signals if, for instance, the two rovibrational transitions induced by the two lasers share a common lower level. Therefore, the OODR spectrum is much simpler than the absorption spectrum. It consists of only four lines for each vibrational band, it is isotope-selective and essentially Doppler-free. However, the OODR lines are power-broadened due to the high laser intensities necessary for obtaining the signals. Using the measured frequency separation $Q(J) - P(J)$ and $R(J) - Q(J)$ of the OODR spectrum the value of J and an approximate value of the rotational constant of the upper state may easily be deduced. By performing OODR investigations for different common lower levels we could successfully assign rotational quantum numbers and branches to the numerous lines of the absorption spectrum as indicated in Fig. 1.

Another source of experimental information on the interatomic potential is an investigation of the spectral distribution of the fluorescence light. The frequency of

the exciting laser is fixed to a proper transition. The fluorescence light is focussed onto the entrance slit of a grating monochromator which is scanned under computer
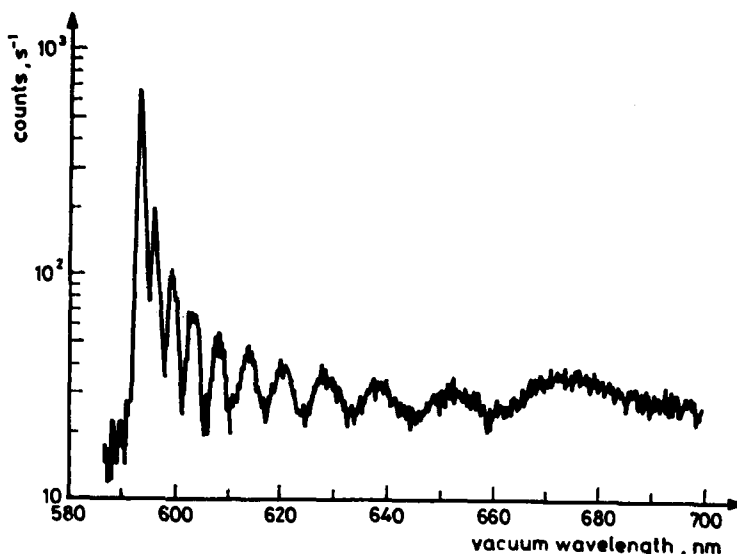

Fig. 2. Spectral intensity distribution of fluorescence light. The laser was tuned to a wavenumber of 16 862.43 cm^{-1} exciting the hfs component $G = 2$ of the $Q_2(9.5)$ line of the transition
$$X^2\Sigma v'' = 0 \rightarrow A^2\Pi_{3/2}v' = 10 \text{ of NaKr}^{84}$$

control by means of a step motor. The result of our measurement in Fig. 2 obtained with an apparatus width of 1 nm shows a pattern with several peaks extending over a wavelength range of about 100 nm. The first peak at low wavelength contains all transitions to bound levels of the molecular ground state, whereas the remaining part of the spectrum is due to bound-free transitions ending on the repulsive part of the interatomic potential of the ground state. The whole pattern shows a clear reflection structure "reflecting" the radial probability distribution of the vibrational wave function of the upper bound state into the observed spectrum. A simple counting of the number of peaks yields then the vibrational quantum number of the upper state.

3. Results

For the case of NaKr our previous investigation of the absorption spectrum of the $A\Pi - X\Sigma$ transition covered the range of wavenumbers between 16 858 and 16 950 cm^{-1}. The present work deals with an extension of this investigation to lower wavenumbers down to 16 758 cm^{-1}. Up to now, our analysis is restricted to the most abundant krypton isotope Kr^{84} with a relative abundance of 57% in

natural mixture of isotopes. We were able to assign rotational quantum numbers and rotational branches to about 700 additional absorption lines of the molecule NaKr[84]. These lines belong to transitions between vibrational levels $v' = 8...10$ of the $A\Pi$ state and $v'' = 0..2$ of the $X\Sigma$ state. The measured frequency positions of these lines were fitted to the proper molecular Hamiltonian together with our previous results in one global fit in order to determine the molecular parameters of rotation, vibration, fine-structure splitting and λ-type doubling.

For the $X\Sigma$ state we obtained for the first time rotationally resolved spectra for the vibrational levels $v'' = 1$ and 2. Our results compiled in Table I allow us a

Table I

Rotational constants and energy differences of vibrational levels
of the $X\Sigma$ state of NaKr[84]

v''	$B_{v''}[GHz]$	$D_{v''}[10^{-5}\ GHz]$	$H_{v''}[10^{-9}\ GHz]$	$(E_{v''+1} - E_{v''})[\ GHz]$
0	1.1285(2)	3.29(4)	$-2.2(2)$	
				396.91(2)
1	1.0645(3)	3.76(7)	$-3.8(6)$	
				348.26(2)
2	1.9940(4)	4.38(18)	$-7.7(2.6)$	

more precise determination of the bound part of the $X\Sigma$ potential than before [2]. This part of the potential may be represented to a good approximation by a Morse potential with an equilibrium distance of 0.4917(2) nm, a well-depth of 68.1(3) cm^{-1} and with $\beta a_0 = 0.493(2)$ (a_0 Bohr radius). Expanding the experimental values of $B_{v''}$ of Table I into a power series with respect to $v'' + 1/2$ the coefficient of the linear term turns out to be $\alpha_e = 0.0576(8)$ GHz. From the Morse potential given above we deduce a value of $\alpha_e = 0.0647$ GHz which is in satisfactory agreement with the experimental results. According to the Morse approximation altogether 9 vibrational levels $v'' = 0...8$ are expected to be bound within the well of the $X\Sigma$ potential.

For the excited $A\Pi$ states we have determined the parameters of rotation, of fine structure splitting and of λ-type doubling for the vibrational levels $v' = 8, 9$ and 10 for the first time. Parts of our results are compiled in Table II. As can be seen

Table II

Fine structure splitting constant A, rotational constant B, and
energy value of vibrational levels of the $A^2\Pi$ state of NaKr[84]

v'	A [GHz]	B [GHz]	$(T_{v'} - T_0)$ [cm^{-1}]
8	938.79(2)	2.1087(3)	16 774.611(4)
9	877.37(2)	1.9974(2)	16 812.721(4)
10	818.26(2)	1.8849(2)	16 846.774(4)

from Table II the fine structure splitting constant increases with decreasing v' and is much higher than the value of 345 GHz expected for a Hund's coupling case a from the fine structure splitting of the 3^2P state of the sodium atom. The interatomic potential of the $A^2\Pi_{1/2}$ and the $A^2\Pi_{3/2}$ state has been obtained in tabulated form by means of the usual RKR procedure using all our data for the vibrational levels

$v' = 8..14$. In comparison with the results of recent model potential calculations
[3] our RKR potential curve is of similar shape, but is shifted by about 0.02 nm to
higher internuclear separations.

As already mentioned, the fluorescence spectrum of Fig. 2 is useful in order
to obtain information on the repulsive part of the $X\Sigma$ potential. We have used
a computer program solving the Schrödinger equation for the upper bound state
and for the lower continuum states for a given tabulated $A\Pi$ and $X\Sigma$ potential,
resp. and calculating the intensity of the fluorescence light as a function of the
wavelength. Using the results of the model potential calculations of Düren et al
[3] for the $A\Pi$ and the $X\Sigma$ potential we found considerable discrepancies between
the calculated pattern and the experimental curve, the experimental maxima oc-
curing consistently at lower wavelengths than in the calculated curve. Therefore,
we changed the repulsive part of the $X\Sigma$ model potential by means of a simple two-
parameter polynomial in R (R internuclear separation). Setting the coefficients
of the polynomial to proper values we obtained better agreement between experi-
ment and calculation. As can be seen from our preliminary results in Table III the
repulsive part of the $X\Sigma$ model potential has to be lowered consirably. However,

Table III

Preliminary results for the repulsive part V
of the $X\Sigma$ potential as a function of R
in comparison with the result V_{mod} of the
model potential calculation [3]

R [nm]	V [cm^{-1}]	V_{mod} [cm^{-1}]
0.265	1484	2192
0.291	712	1284
0.330	399	653
0.370	218	270
0.410	52	53

we could not obtain full agreement between experiment and calculation with this
simple modification and a more refined analysis is certainly necessary.

4. Local perturbation

For increasing vibrational quantum number v' in the $A\Pi$ state the energy
values of the levels v' of the $A\Pi_{3/2}$ and $v' + 1$ of the $A\Pi_{1/2}$ approach each other. Due
to the different rotational constants in both levels we get a crossing of the two
rotational ladders at a certain non-integer value of the rotational quantum number.
The energy values of the rovibrational levels near the crossing point are considerably
shifted by the non-diagonal part of the rotational Hamiltonian proportional to the
operator $J_+S_- + J_-S_+$ ($\vec{J}, \vec{S}$ operator of total and spin angular momentum, resp.).
This operator connects the rovibrational levels v', J' of the $A\Pi_{3/2}$ state and $v'+1, J'$
of the $A\Pi_{1/2}$ state. However, its effect is only important close to the crossing
and may be neglected far away from the crossing. In the experimental absorption

spectrum the local perturbation shows up as a shift of the corresponding absorption lines from their regular positions.

A full deperturbation analysis has already been performed for the local perturbation between $v' = 11$, $\Omega = 3/2$ and $v' = 12$, $\Omega = 1/2$ as well as between $v' = 12$, $\Omega = 3/2$ and $v' = 13$, $\Omega = 1/2$ in NaKr [2]. Therefore, I restrict myself to our new results for the case of NaAr. A local perturbation occurs between the levels $v' = 11$, $\Omega = 3/2$ and $v' = 12$, $\Omega = 1/2$ around $J' = 11.5$. In order to get a rotational assignment for the molecular absorption lines near the local perturbation where the spectrum is highly congested it was necessary to perform OODR investigations. By means of these investigations we were able to determine the positions of about 30 absorption lines with known assignment near the local perturbation and to deduce preliminary values of the perturbation parameter $B(v', v' + 1)$. Using this preliminary result we could identify about 70 molecular absorption lines in the absorption spectrum due to the transitions $A\Pi_{3/2}$, $v' = 11 - X\Sigma v'' = 0$ and $A\Pi_{1/2}$, $v' = 12 - X\Sigma v'' = 0$ with J'' - values ranging up to 17.5.

Finally, we performed successfully a deperturbation analysis using the same procedure as described in [2]. The rotational perturbation parameter was determined to be $B_{11/12} = 0.474(3)$ GHz for the $A\Pi$ state of NaAr. The perturbation is slightly different for e and f levels. This effect may be taken into account by introducing a second phenomenological parameter $q(v', v' + 1)$ into the Hamilton operator of the perturbation [2]. For the case of the $A\Pi$ state of NaAr we obtain $q_{11/12} = 0.021(5)$ GHz. Our experimental results for $B_{11/12}$ may be compared to the theoretical prediction which is proportional to the matrix element of $1/R^2$ between the two vibrational states. The vibrational wavefunctions have been calculated by solving the Schrödinger equation of molecular vibration using the model potential of Düren et al [3] for the interatomic potential of the $A\Pi$ state. The result of this calculation is $B_{11/12} = 0.505$ GHz which is in very good agreement with the experimental value.

References

1. G. Aepfelbach, A. Nunnemann and D. Zimmermann, Chem. Phys. Lett., *96*, 311, 1983.
2. E. Zanger, V. Schmatloch and D. Zimmermann, J. Chem. Phys., *88*, 5396, 1988.
3. R. Düren, E. Hasselbrink and G. Moritz, Z. f. Physik, *A307*, 1, 1982; R. Düren and E. Hasselbrink, private communication, 1981.